On the anomalous vibron-phonon dispersion in solid tetracyanoethene, $C_2(CN)_4$

1989 J. Phys.: Condens. Matter 1 4047

(http://iopscience.iop.org/0953-8984/1/26/002)

J. Phys.: Condens. Matter 1 (1989) 4047–4055. Printed in the UK

On the anomalous vibron–phonon dispersion in solid tetracyanoethene, $C_2(CN)_4$

Tom H M van den Berg and Ad van der Avoird
Institute of Theoretical Chemistry, University of Nijmegen, Toernooiveld, Nijmegen, The Netherlands

Received 25 November 1988, in final form 31 January 1989

Abstract. The anomalous dispersion found by inelastic neutron scattering in one of the vibron bands in solid tetracyanoethene appears to be due to the electrostatic interactions that couple the infrared-active intramolecular vibrations via the transition dipole resonance mechanism. This is demonstrated by way of both numerical lattice dynamics calculations and a simple mathematical analysis, which relates the Fourier components of the dispersion curves in specific directions of the wavevector $\boldsymbol{k}$ to two-dimensional lattice sums over the dipole–dipole interactions between layers perpendicular to $\boldsymbol{k}$. Only for specific orientations of the molecular transition dipole moments in a solid and for specific directions of $\boldsymbol{k}$ will this lead to a dispersion curve of irregular shape.

1. Introduction

Tetracyanoethene (TCNE), being one of the strongest π-electron acceptors commonly used in electron donor/acceptor complexes, has been studied extensively. Several of these studies address the vibrational spectrum of TCNE (Miller *et al* 1964, Takenaka and Hayashi 1964, Rosenberg and Devlin 1965, Popov *et al* 1966, Hinkel and Devlin 1973, Yokoyama and Maeda 1980, Michaelian *et al* 1982), both in solution and in the crystalline state. A wide-ranging experimental and theoretical study of the lattice vibrations (phonons) and the coupled internal vibrations (vibrons) in solid TCNE has been made by Chaplot *et al* (1983). These authors have measured phonon and vibron dispersion relations by inelastic neutron scattering and they have calculated the corresponding dispersion curves by lattice dynamics methods, using a simplified force field for the lowest intramolecular vibrations and an empirical atom–atom potential for the intermolecular interactions. Generally, the calculated dispersion relations agree well with experiment provided that the mixing between the lowest internal vibrations and the lattice vibrations is taken into account.

One of the branches showed an unusually strong dispersion, however, which has been determined both by constant-wavevector scans and by constant-energy scans with the triple-axis neutron spectrometer, but which is not reproduced in any way by the calculations. The calculations gave a smooth and rather flat energy dependence for this branch with no sign of the observed anomalous dispersion, even when phonon–vibron mixing and the mixing between the vibron modes associated with different internal vibrations were included. Chaplot *et al* (1983) speculated that the electrostatic inter-

0953-8984/89/264047 + 09 $02.50

Table 1. Free molecular vibrations of TCNE.

Symmetry (D_{2h})	Frequency (cm^{-1})† VFF	Rigid C—C≡N model	Observed IR/Raman spectra	Character of normal mode
b_{2u}	81	74		(NC)—C—(CN) rocking
a_u	88	74		C=C torsion
a_g	133	102	130	(NC)—C—(CN) scissoring
b_{3u}	146	152	180	(NC)—C—(CN) wag
b_{1u}	182	154	165	(NC)—C—(CN) scissoring
b_{3g}	239	250	254	(NC)—C—(CN) rocking
b_{2g}	260	353	251	(NC)—C—(CN) wag
b_{1g}	375	—	360	C—C≡N bend (out-of-plane)
a_u	425	—	410	C—C≡N bend (out-of-plane)
b_{2u}	440	—	443	C—C≡N bend (in plane)
b_{3g}	452	—		C—C≡N bend (in plane)
a_g	489	—	490	C—C stretch/C—C≡N bend
b_{3u}	524	—	555	C—C≡N bend (out-of-plane)
b_{1u}	559	—	579	C—C≡N bend (in plane)
a_g	559	—	535	C—C stretch/C—C≡ bend
b_{2g}	682	—	674	C—C≡N bend (out-of-plane)
b_{1u}	956	—	958	C—C stretch
b_{2u}	1152	—	1155	C—C stretch
b_{3g}	1278	—	1282	C—C stretch
a_g	1571	—	1569	C=C stretch
b_{1u}	2231	—	2230	C≡N stretch
a_g	2235	—	2235	C≡N stretch
b_{2u}	2253	—	2263	C≡N stretch
b_{3g}	2256	—	2247	C≡N stretch

† 1000 cm^{-1} = 29.98 THz.

actions, which had not been included in the lattice dynamics calculations, might be responsible for this anomalous dispersion. In the present paper we shall show explicitly the effects of including the electrostatic interactions and the use of a more realistic intramolecular force field. We shall demonstrate the physical explanation for the anomalous dispersion and discuss the conditions for which this phenomenon can occur in TCNE, as well as in other systems.

2. Internal vibrations

Empirical valence force fields (VFF) (Hinkel and Devlin 1973, Michaelian *et al* 1982) and Urey–Bradley force fields (Takenaka and Hayashi 1964, Rosenberg and Devlin 1965, Yokoyama and Maeda 1980) for the free molecular vibrations in TCNE have been determined from the experimental infrared and Raman spectra. In our calculations we have used the VFF parameters of Hinkel and Devlin (1973) for the in-plane vibrations and those of Michaelian *et al* (1982) for the out-of-plane motions. The molecular vibrational frequencies and the corresponding normal mode eigenvectors have been determined by the standard ***GF*** matrix method (Wilson *et al* 1955). We observe (see table 1) that the

seven lowest-frequency vibrations do indeed correspond to the scissoring, rocking, wagging and torsional motions of the (NC)—C—(CN) groups, but also that the C—C≡N bending motions admix to a considerable extent. For instance, in the b_{3u} wagging mode discussed in § 4, the C—C bonds bend out of the molecular plane by 1.5° (C═(C < $^{C}_{C}$) wagging angle 3.0°), but the C—C≡N groups also bend by 1.5°. In other words the C—C≡N groups do not really behave as rigid units in these low-frequency vibrations. We have also simulated the rigid C—C≡N model of Chaplot *et al* (1983) by making all stretch force constants and the C—C≡N bending force constant infinitely high and adapting the remaining VFF constants to obtain practically the same frequencies as Chaplot *et al* (1983). The eigenvectors are completely determined by symmetry in this model, but some of the frequencies differ considerably from those obtained in the complete VFF model (see table 1). This confirms the non-rigid nature of the C—C≡N groups in the low-frequency modes.

3. Lattice dynamics calculations

The calculations of the phonon and vibron dispersion relations are based on the standard harmonic lattice dynamics method, as extended to internal vibrations by Taddei *et al* (1973) and Califano *et al* (1981). We include the full self-term (Neto *et al* 1976, Neto and Kirin 1979), in order to ensure complete translational and rotational invariance of the harmonic lattice Hamiltonian. For the internal vibrations we use the normal mode eigenvectors from the free molecular calculations (described in § 2), transformed from a molecular system of axes to the crystal frame. The calculated free molecule frequencies are replaced by experimental values, as far as available (see table 1).

The intermolecular potential is represented by an atom–atom potential $V(r) = B_{ij}\exp(-C_{ij}r) - A_{ij}r^{-6} + q_iq_jr^{-1}$ with the same parameters A_{ij}, B_{ij} and C_{ij} as used by Chaplot *et al* (1983). The electrostatic interactions have been added, however, and the fractional atomic charges q_i have been determined by the following procedure. Given the charge neutrality of the TCNE molecule as a whole and its D_{2h} symmetry, only two parameters q_i can be determined independently. These parameters can be obtained from the quadrupole moment tensor of the molecule which has also two independent components. Calculating the quadrupole moment of TCNE by means of *ab initio* LCAO-SCF calculations in one of the standard AO basis sets with the program GAMESS (Dupuis *et al* 1980) yields $q_C = -0.190e$, for the C═C carbon atoms, $q'_C = +0.489e$ for the C≡N carbon atoms and $q_N = -0.394e$, if the split-valence 3-21G basis is used (and not very different values for the minimal STO-3G basis). Since later in this paper we shall concentrate on the b_{3u} out-of-plane (NC)—C—(CN) wagging mode, we have also made *ab initio* calculations for TCNE deformed along the normal coordinate of this mode. Thus, we could calculate numerically the dipole moment derivative along the b_{3u} wagging mode and compare the *ab initio* value with the value derived from the point charges obtained previously. The agreement is reasonably good: the point-charge model adapted to the static quadrupole tensor yields a dipole derivative which is 20% too large (or 20% too small if we use the normal coordinate of the simplified wagging model with rigid C—C≡N groups). Furthermore, we have found that even the changes in the quadrupole moment upon deformation are reasonably well represented by the point-charge model. So we use these point charges† to represent the electrostatic interactions between the

† Another way to obtain fractional atomic charges from *ab initio* LCAO-SCF calculations proceeds via a Mulliken population analysis. It is well known among quantum chemists, however, that the Mulliken atomic charges form a poor representation of the electrostatic interactions. We have also reached this conclusion in the present case.

molecules and their dependence on the internal vibrations. Before performing the actual lattice dynamics calculations we optimised the unit cell parameters and the molecular orientations. Addition of the electrostatic interactions to the intermolecular potential did not significantly change the optimised crystal geometry already calculated by Chaplot *et al* (1983), except that the unit cell becomes slightly too compact. We would have to re-optimise the empirical parameters A_{ij}, B_{ij} and C_{ij} in the atom–atom potential, after the addition of the electrostatic interactions, in order to recover the correct unit cell volume.

4. Vibron and phonon dispersion relations

Neutron scattering experiments (Chaplot *et al* 1983) were performed on TCNE in the monoclinic phase, space group $P2_1/n$, supercooled to 5 K. The two molecules in the unit cell are centred at (0, 0, 0) and ($a/2$, $b/2$, $c/2$), respectively, and they are related by a screw axis 2_1 along the $\boldsymbol{b}$ direction and a glide plane parallel to the $\boldsymbol{ac}$ plane. We use the same convention as Chaplot *et al* (1983) for displaying the phonon and vibron dispersion curves along the $\boldsymbol{a}^*$, $\boldsymbol{b}^*$ and $\boldsymbol{c}^*$ directions of the Brillouin zone and defining the symmetry of the normal modes with respect to the screw axis and the glide plane.

When we omit the electrostatic interactions from our calculations, we obtain practically the same dispersion curves as Chaplot *et al* (1983) for the lowest 26 modes, which originate from the three translational vibrations, three librations and the lowest seven internal vibrations of the two molecules in the unit cell. So the use of non-rigid C—C≡N groups in the intramolecular force field practically does not influence the dispersion relations at this level. (We shall later observe that it does when the electrostatic interactions are included.) Apart from the anomalous dispersion along the $\boldsymbol{a}^*$ direction observed in the mode around 5.5 THz, the agreement with the experimental dispersion curves shown in figure 1 is rather good and we obtain substantial mixing between the highest lattice modes and the lowest internal modes, just as found by Chaplot *et al* (1983).

The addition of electrostatic interactions through the point-charge model discussed in § 3 yields the dispersion curves shown in figure 2. Although most of the phonon/vibron dispersion curves are not much affected, their resemblance to the experimental picture (figure 1) becomes slightly better in general. All the frequencies are too high, however, which is due to the compactness of the unit cell calculated with the point charges without re-optimising the remainder of the atom–atom potential. Also we find too strong a dispersion of some of the higher modes in figure 2 along the $\boldsymbol{b}^*$ direction, which is due to artificial mixing between these modes, some of which are raised more than others.

Let us now concentrate on the mode around 5.5 THz in figure 1 (experimental), which displays the anomalous dispersion in the $\boldsymbol{a}^*$ direction. In figure 2 (calculated) this mode lies around 7 THz and we clearly observe an irregular shape of its dispersion curve along the $\boldsymbol{a}^*$ direction which resembles the shape of the experimental curve. Since the corresponding curve calculated without the addition of point charges to the atom–atom potential is completely structureless, as in Chaplot *et al* (1983), we conclude that the anomalous dispersion of this branch is indeed caused by the electrostatic interactions between the molecules. In § 5, we shall investigate its shape and its physical origin in more detail. First we establish, by inspecting the eigenvector of the mode which displays the anomalous dispersion, that this mode is purely the b_{3u} out-of-plane wagging mode of the TCNE molecules. Inclusion of just this mode in the lattice dynamics model yields

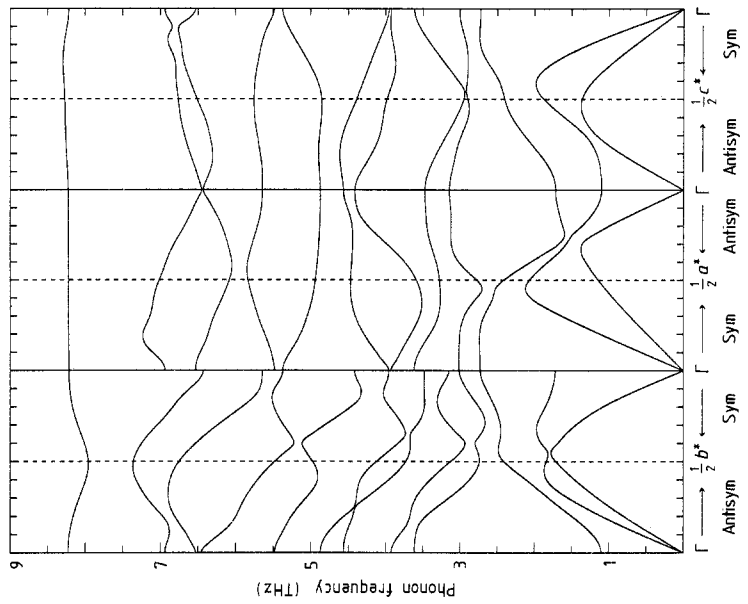

Figure 2. Phonon–vibron dispersion relations in monoclinic TCNE from lattice dynamics calculations, using an atom–atom potential supplemented by electrostatic interactions between fractional atomic charges (see § 4 of text). Lattice sums over the intermolecular interactions have been taken up to $R = 30$ Å.

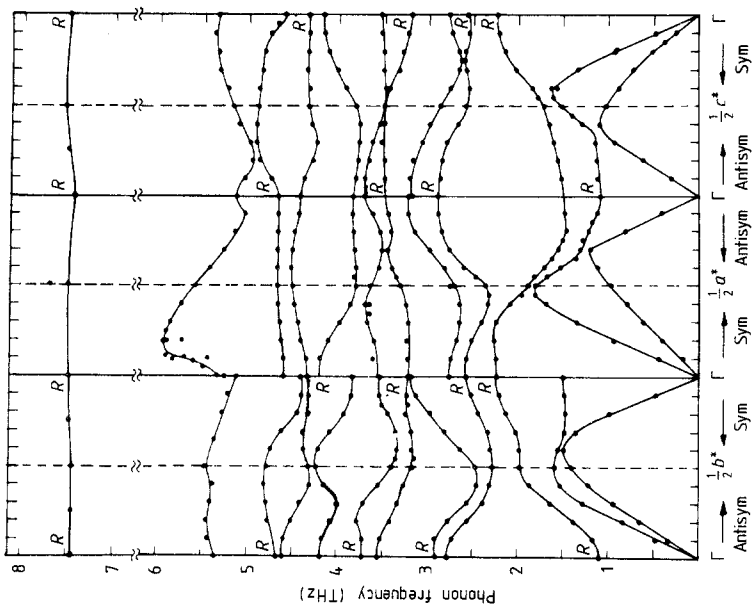

Figure 1. Experimental phonon–vibron dispersion relations in the monoclinic phase of TCNE, obtained from coherent inelastic neutron scattering by Chaplot *et al* (1983).

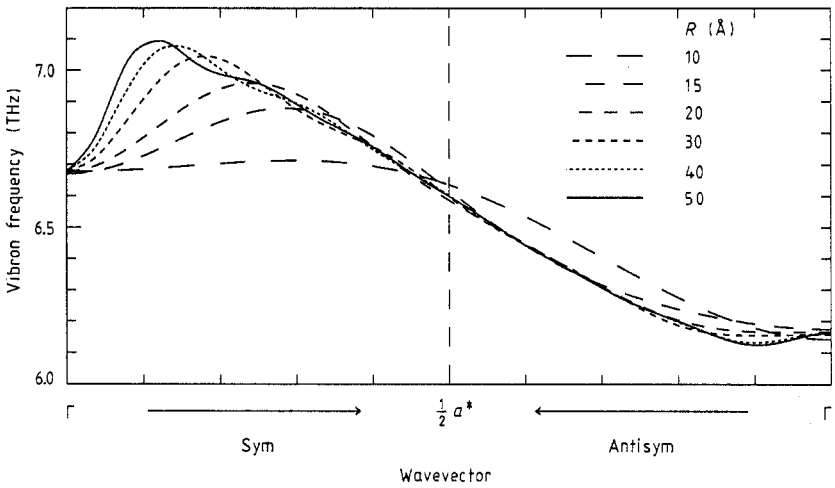

Figure 3. Vibron dispersion of the b_{3u} out-of-plane wagging mode from lattice dynamics calculations, using the atom–atom potential with the fractional atomic charges. The dispersion curves for wavevectors $\boldsymbol{k}$ along the $\boldsymbol{a}^*$ direction in the Brillouin zone of the vibron modes that are symmetric/antisymmetric with respect to the crystal glide plane are shown for an increasing radius R of truncation of the lattice sums.

the dispersion curve shown in figure 3, which is practically identical to the curve from the complete calculation, if we take the same radius of truncation (R = 30 Å) of the lattice sum over the intermolecular interactions. So the effects of phonon–vibron mixing or mixing between different internal vibrations which, via avoided crossings, are known to yield rather typical dispersion behaviour in many instances, are not relevant in this case. On the other hand, we observe that the shape of the unusual dispersion curve is very sensitive to changes of the fractional atomic charges and to an increase of the radius of truncation of the lattice sum. The dispersion curve in figure 3 calculated with the largest radius, R = 50 Å, shows a striking similarity in shape to the experimental curve, shown in detail in figure 4. This shape is also altered by replacement of the intramolecular wagging eigenvector from the complete VFF calculation by the eigenvector from the simplified model with rigid C—C≡N groups. By means of a further analysis of the calculated and experimental dispersion curves in § 5, we conclude that the coupling between the intramolecular wagging vibrations which leads to the unusual dispersion of the corresponding vibron band in the $\boldsymbol{a}^*$ direction is due to transition dipole–dipole interactions. As is shown by its strong infrared activity (Chaplot *et al* 1983), the transition dipole moment associated with the b_{3u} out-of-plane wagging vibration is indeed large. We next discuss the conditions under which such a large transition dipole moment can cause unusual dispersion relations.

5. Anomalous vibron dispersion from transition dipole–dipole coupling

From the observation that vibron dispersion curves are mostly rather smooth and flat, except near avoided crossings, it may be concluded that the mere occurrence of relatively large vibrational transition dipole moments is not sufficient to cause such a strong

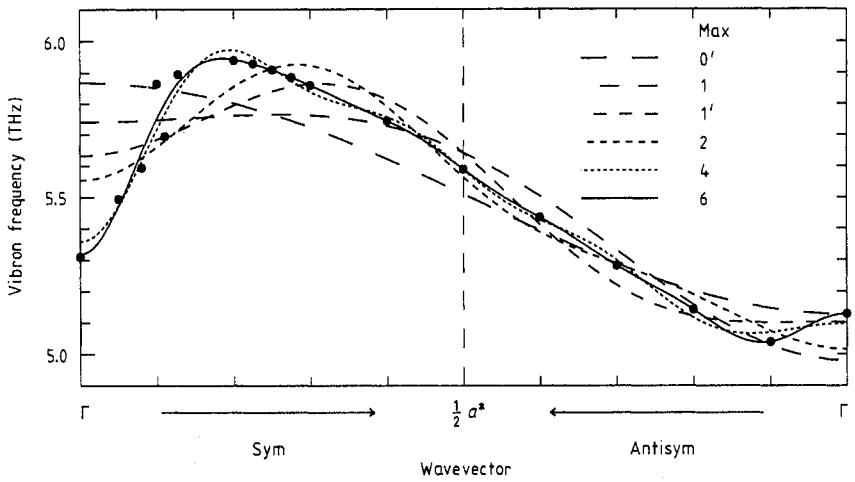

Figure 4. Fourier analysis of the experimental vibron branch in figure 1 which shows the anomalous dispersion. The curves marked in the key include higher and higher Fourier components $\cos(\frac{1}{2}mkd/2)$. As explained in the text, these Fourier components correspond to the intermolecular couplings between crystal layers perpendicular to the a^* axis with increasing distances $\frac{1}{2}md$, where $m = 1, 2, 3, 4, 8$ and 12 (e.g. max = 1′ corresponds to a maximum value $m = 3$).

dispersion as found in one particular vibron band of solid TCNE. Here we investigate the required additional conditions.

A quantum mechanical system of molecules that vibrate in a single normal mode with (unperturbed) frequency ω_0, which are coupled via transition dipole–dipole interactions, may be replaced (in the sense that it has the same dispersion relations) by a model of oscillating dipoles with eigenfrequency ω_0 that interact via classical dipole–dipole interactions. Let us take a lattice of such dipoles with two equivalent sublattices, as is the case in solid TCNE. The transition dipole moment for the b_{3u} out-of-plane wagging mode in TCNE lies perpendicular to the molecular plane. So the molecular orientations in the solid fix the directions (ϑ, φ) and (ϑ', φ') of the oscillating dipole moments in the two sublattices. The dipole moments are written as $\boldsymbol{\mu} = (\partial\boldsymbol{\mu}/\partial Q)Q$, where Q is the normal coordinate of the free molecule vibration. This yields the dispersion relations

$$\omega_{\pm}^2(\boldsymbol{k}) = \omega_0^2 + A(\boldsymbol{k}) \pm A'(\boldsymbol{k}) \tag{1}$$

where $A(\boldsymbol{k})$ and $A'(\boldsymbol{k})$ are the intra- and inter-sublattice couplings between Bloch waves of oscillating dipoles with wavevector $\boldsymbol{k}$. For a given direction of $\boldsymbol{k}$ in the Brillouin zone (for instance, either one of the $\boldsymbol{a}^*$, $\boldsymbol{b}^*$ and $\boldsymbol{c}^*$ directions shown in figures 1 and 2), we can write

$$\begin{aligned} A(\boldsymbol{k}) &= F_{00} + 2\sum_{n=1}^{\infty} F_{0n}\cos(knd) \\ A'(\boldsymbol{k}) &= 2\sum_{n'=0}^{\infty} F_{0n'}\cos[k(n'd + d')] \end{aligned} \tag{2}$$

where k is the length of the vector $\boldsymbol{k}$. The labels n and n' run over layers perpendicular to the wavevector $\boldsymbol{k}$. The layers n are of the same sublattice as the layer $n = 0$, the layers

n' belonging to the other sublattice; d is the distance between subsequent layers of the same sublattice and d' is the distance between layer $n = 0$ and the nearest layer of the other sublattice. The quantities F_{0n} and $F_{0n'}$ are two-dimensional lattice sums over layers perpendicular to $\boldsymbol{k}$, which can be expanded in a two-dimensional Fourier series (Steele 1973)

$$F_{0n} = \sum_{g} v_n(\boldsymbol{g}) \exp(\mathrm{i}\boldsymbol{g} \cdot \boldsymbol{\tau}_n)$$
$$F_{0n'} = \sum_{g} v_{n'}(\boldsymbol{g}) \exp(\mathrm{i}\boldsymbol{g} \cdot \tau_{n'}). \tag{3}$$

For a lattice of interacting dipoles, the Fourier coefficients can be evaluated analytically (Nijboer and De Wette 1958):

$$v_n(\boldsymbol{g}) = (2\pi|\partial\boldsymbol{\mu}/\partial Q|^2/\sigma_c)\, B(\vartheta, \varphi, \vartheta, \varphi, \varphi_g) \exp(-gnd)$$
$$v_{n'}(\boldsymbol{g}) = (2\pi|\partial\boldsymbol{\mu}/\partial Q|^2/\sigma_c)\, B(\vartheta, \varphi, \vartheta', \varphi', \varphi_g) g \exp[-g(n'd + d')]. \tag{4}$$

The vectors $\boldsymbol{\tau}_n$ and $\boldsymbol{\tau}_{n'}$ describe the parallel displacements of the layers relative to the layer $n = 0$. The vector $\boldsymbol{g}$ is a two-dimensional reciprocal lattice vector perpendicular to $\boldsymbol{k}$, g is the length of this vector, φ_g its direction and σ_c the area of the two-dimensional unit cell. The function B equals -1 in the special case treated by Nijboer and De Wette (1958). In general, it depends on the polar angles (ϑ, φ) and (ϑ', φ'), which describe the orientations of the dipole moments in the two sublattices, relative to a frame which has its z axis parallel to the wavevector $\boldsymbol{k}$:

$$B(\vartheta_1, \varphi_1, \vartheta_2, \varphi_2, \varphi_g) = [\sin\vartheta_1 \cos(\varphi_g - \varphi_1) + \mathrm{i}\cos\vartheta_1]$$
$$\times [\sin\vartheta_2 \cos(\varphi_g - \varphi_2) + \mathrm{i}\cos\vartheta_2]. \tag{5}$$

For specific directions of the wavevector $\boldsymbol{k}$ the crystal symmetry, i.e. the screw axis or the glide plane, will induce special relations between (ϑ, φ) and (ϑ', φ').

According to equations (1) and (2), the intra- and inter-sublattice coupling constants F_{0n} and $F_{0n'}$, which are given by equations (3) to (5), are the Fourier components of the dispersion curves $\omega_+(k)$ and $\omega_-(k)$, considered along specific directions of the wavevector $\boldsymbol{k}$. In figure 4 we show a Fourier analysis of the experimental dispersion curve for $\boldsymbol{k}$ along the $\boldsymbol{a}^*$ direction, which displays the anomalous dispersion. We observe that rather high Fourier components contribute to this curve, which is not surprising given its irregular shape. The same effect is shown by the calculated results in figure 3: the dispersion curve associated with the b_{3u} wagging mode becomes more and more irregular when it is calculated with an increasing radius of summation of the intermolecular interactions. The increase of this radius implies, of course, that more and more interlayer couplings F_{0n} and $F_{0n'}$ and, therefore, higher Fourier components are taken into account. The shape of the curve calculated with the largest radius of summation is strikingly similar to that of the experimental curve. In order to obtain the exact result we have to invoke the Ewald method (Born and Huang 1954).

6. Conclusion

Through *ab initio* calculations we have obtained a fractional atomic charge model for TCNE, which yields a good representation of the electrostatic intermolecular interactions, as well as a fairly good transition dipole moment for the b_{3u} out-of-plane wagging

vibration in which we are especially interested. We have refined the lattice dynamics calculations of Chaplot *et al* (1983) on solid TCNE, by addition of the interaction between these charges to the usual atom–atom potential and by the use of a more realistic force field for the internal molecular vibrations. The latter refinement did not prove essential for the shape of the vibron dispersion curves (although it changes the vibrational frequencies considerably), but the addition of the electrostatic interactions shows clearly that the anomalous vibron dispersion found by inelastic neutron scattering for the b_{3u} wagging mode is due to strong transition dipole–dipole coupling. In a further analysis we have established that this coupling will only lead to such an irregular shape of the vibron dispersion curve for specific orientations of the molecular transition dipole moments in the two sublattices of TCNE and for specific directions of the wavevector $\boldsymbol{k}$. The observed hump in the dispersion curve is due to the relative importance of high Fourier coefficients, which are given as two-dimensional lattice sums for the dipole–dipole interactions between different crystal layers perpendicular to the wavevector $\boldsymbol{k}$.

Acknowledgments

We thank Dr A Mierzejewski for suggesting this problem and Professor T Luty for discussions. This investigation was supported partly by the Netherlands Foundation for Chemical Research (SON) with financial aid from the Netherlands Organization for the Advancement of Research (NWO).

References

Born M and Huang K 1954 *Dynamical Theory of Crystal Lattices* (Oxford: Clarendon)
Califano S, Schettino V and Neto N 1981 *Lattice Dynamics of Molecular Crystals* (Berlin: Springer)
Chaplot S L, Mierzejewski A, Pawley G S, Lefebvre J and Luty T 1983 *J. Phys. C: Solid State Phys.* **16** 625
Dupuis M, Spangler D and Wendoloski J J 1980 *NRCC PROGRAM QG01*
Hinkel J J and Devlin J P 1973 *J. Chem. Phys.* **58** 4750
Michaelian K H, Rieckhoff K E and Voigt E M 1982 *J. Mol. Spectrosc.* **95** 1
Miller F A, Sala O, Devlin P, Overend J, Lippert E, Luder W, Moser W and Varchmin J 1964 *Spectrochim. Acta* **20** 1233
Neto N and Kirin D 1979 *Chem. Phys.* **44** 245
Neto N, Taddei G, Califano S and Walmsley S H 1976 *Mol. Phys.* **31** 457
Nijboer B R A and De Wette F W 1958 *Physica* **24** 422
Popov E M, Yakovlev I P, Kogan G A and Zhogina V V 1966 *Teor. Eksp. Khim.* **2** 464
Rosenberg A and Devlin P J 1965 *Spectrochim. Acta* **21** 1613
Steele W A 1973 *Surf. Sci.* **36** 317
Taddei G, Bonadeo H, Marzocchi M P and Califano S 1973 *J. Chem. Phys.* **58** 966
Takenaka T and Hayashi S 1964 *Bull. Chem. Soc. Japan* **37** 1216
Wilson E B, Decius J C and Cross P C 1955 *Molecular Vibrations* (New York: McGraw Hill)
Yokoyama K and Maeda S 1980 *Bull. Chem. Soc. Japan* **53** 1949